ACS Catalysis

Research Article

pubs.acs.org/acscatalysis

Immobilizing Ru(bda) Catalyst on a Photoanode via Electrochemical Polymerization for Light-Driven Water Splitting

Fusheng Li,[†] Ke Fan,[†] Lei Wang,[†] Quentin Daniel,[†] Lele Duan,[†] and Licheng Sun*[,†,‡]

[†]Department of Chemistry, KTH-Royal Institute of Technology, Teknikringen 30, 10044 Stockholm, Sweden

[‡]State Key Laboratory of Fine Chemicals, DUT-KTH Joint Education and Research Center on Molecular Devices, Dalian University of Technology (DUT), Dalian 116024, People's Republic of China

Supporting Information

ABSTRACT: The molecular water oxidation catalyst **1** was electrochemically polymerized on a dye-sensitized TiO_2 electrode and an Fe_2O_3 nanorod electrode. High photocurrent densities of ca. 1.4 mA cm^{-2} for poly-**1**+**RuP**@TiO_2 and ca. 0.4 mA cm^{-2} for poly-**1**@Fe_2O_3 were achieved under pH-neutral conditions. A kinetic isotope effect (KIE) study on poly-**1**+**RuP**@TiO_2 shows that poly-**1** catalyzes water oxidation on the surface of TiO_2 via a radical coupling mechanism.

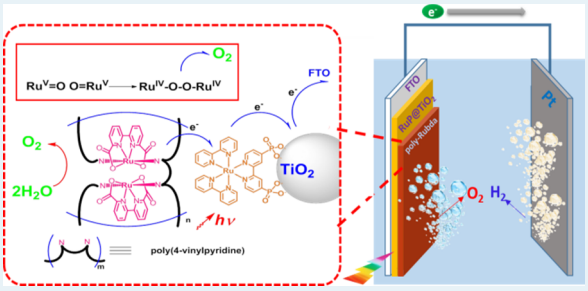

KEYWORDS: *water oxidation, photoanode, light-driven water splitting, molecular catalyst, polymer*

To satisfy the world demand for sustainable energy systems, utilization of solar energy to produce hydrogen by photoelectrochemical (PEC) cells is one of the most promising technical routes.[1−3] Molecular catalysts show a great potential for high-performance water splitting devices due to their relatively easy tunability and high activity.[4−8] We have recently developed a series of ruthenium water oxidation catalysts (WOCs) [Ru(bda)L_2] (bda^{2-} = 2,2′-bipyridine-6,6′-dicarboxylate; L = N-cyclic aromatic ligands, such as pyridine and imidazole),[9−13] and these catalysts show extremely high activities for water oxidation driven by the strong oxidizing reagent $(NH_4)_2Ce(NO_3)_6$ (Ce^{IV}) in pH 1.0 aqueous solutions. Once an efficient catalyst is discovered, one can immobilize on the electrode surface for construction of a PEC cell for water splitting.

With the efficient Ru(bda) WOCs in hand, we constructed a TiO_2/**RuP**/Nafion/Ru(bda) photoanode (**RuP** = [Ru(bpy)$_2$(4,4′-$(PO_3H_2)_2$bpy)]$^{2+}$), in which the Ru(bda) catalyst was encapsulated in Nafion film and achieved light-driven water oxidation.[14] Subsequently, phosphonic acid and silane groups were introduced on Ru(bda) catalysts as anchoring groups for the attachment of Ru(bda) catalysts on the **RuP**-sensitized TiO_2 films via chemical bonds.[15,16] The resulting photoanode gave significantly high photocurrent density for water splitting. Since the Ru(bda) WOCs catalyze water oxidation via a bimolecular reaction mechanism and the rate-determining step of the catalytic cycle is the dimerization of two Ru^V=O species,[11] immobilization of mononuclear Ru(bda) WOCs on the electrode surface disfavors the bimolecular pathway.[15,16] Accordingly, we synthesized a bimolecular Ru(bda) catalyst with an anchoring group and coadsorbed it on the TiO_2 film together with **RuP**, achieving an enhanced photoanode performance.[17] However, the synthetic procedures for the binuclear Ru(bda) catalyst are complicated. To simplify the procedures for immobilization of molecular catalyst on the electrode surface and to facilitate the radical coupling pathway for water oxidation, we herein report a modified Ru(bda) catalyst [Ru(bda)(vpy)$_2$] (**1**; vpy = 4-vinylpyridine) (as shown in Scheme 1) and its facile and efficient immobilization on nanoporous TiO_2 and Fe_2O_3 films via electrochemical polymerization.

The catalyst **1** was prepared by a simple, microwave-assisted, one-pot reaction via self-assembly of three reagents: bda^{2-} (generated in situ by reaction of H_2bda and triethylamine),

Scheme 1. Chemical Structures of Complexes

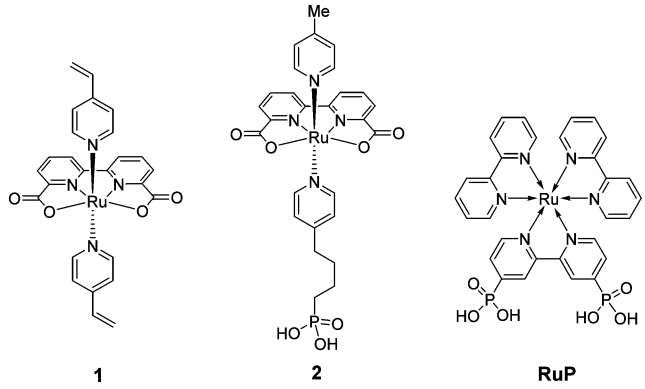

Received: December 30, 2014
Revised: April 2, 2015
Published: May 13, 2015

DOI: 10.1021/cs502115f
ACS Catal. 2015, 5, 3786−3790

$Ru(DMSO)_4Cl_2$, and 4-vinylpyridine. To prepare the photoanode, catalyst **1** was electrochemically polymerized on the **RuP**-sensitized TiO_2 film by electrolysis of an acetonitrile solution of catalyst **1** at −2.0 V (vs $Ag/AgNO_3$) for 200 s, which is a well-known electrochemical method. The polymer will deposit on the electrode surface due to the decrease of solubility.[18−20]

After the polymerization of catalyst **1** on **RuP**@TiO_2, the prepared poly-**1**+**RuP**@TiO_2 electrode was dark red (Figure 1 inset), while the **RuP**@TiO_2 electrode was yellow. The difference in colors strongly indicates the formation of the catalyst polymer in the case of the poly-**1**+**RuP**@TiO_2 electrode. According to the EDX study (Figures S6 and S7 in the Supporting Information), the amount of Ru of poly-**1**+**RuP**@TiO_2 obviously increased in comparison with that of **RuP**@TiO_2. For a comparison with a mononuclear Ru(bda) catalyst photoanode, a **2**+**RuP**@TiO_2 electrode was also prepared (details in the Supporting Information). A cyclic voltammogram (CV) of the **2**+**RuP**@TiO_2 electrode (Figure S10 in the Supporting Information) displays a redox peak of Ru^{II}/Ru^{III} at 0.65 V vs NHE followed by a catalytic water oxidation wave with the onset potential E_{onset} = 1.1 V vs NHE. For poly-**1**+**RuP**@TiO_2 a clear redox peak of Ru^{II}/Ru^{III} can be observed at 0.70 V vs NHE, followed by a catalytic wave with E_{onset} = 1.15 V. In addition to the Ru^{II}/Ru^{III} peak at 0.65 V, the differential pulse voltammogram (DPV) of **2**+**RuP**@TiO_2 (Figures S8 and S9 in the Supporting Information) also resolved the Ru^{III}/Ru^{IV} peak at 0.82 V and displayed an overlap of the peaks Ru^{II}/Ru^{III}(**RuP**) and Ru^{IV}/Ru^{V}(**2**) at around 1.3 V. However, the poly-**1**+**RuP**@TiO_2 electrode had an Ru^{II}/Ru^{III} peak at 0.70 V and an Ru^{III}/Ru^{IV} peak at 0.89 V, following a Ru^{II}/Ru^{III} peak of **RuP** overlapping with Ru^{IV}/Ru^{V}(1.1 V) peak of Ru(bda). The positive potential shift of poly-**1** is due to the coordination of CH_3CN, which was used as a solvent during the polymerization (Figures S1 and S8 in the Supporting Information). This phenomenon is in agreement with our previous studies.[9] These electrochemical results imply that thermodynamically a photogenerated $\mathbf{Ru^{III}P}$ can oxidize the catalyst from Ru^{II} to $Ru^{III}-H_2O$, $Ru^{IV}-OH$ and even to $Ru^{V}=O$ species. In our earlier studies the dinuclear Ru(bda) complex linked with 1,3-bis(pyridin-4-yl)propane went through first-order kinetics for water oxidation,[13] indicating a radical coupling mechanism for catalytic water oxidation. In this work, poly-**1** can be considered as a polymer of the dinuclear Ru(bda) complex, which is beneficial for the radical coupling mechanism.

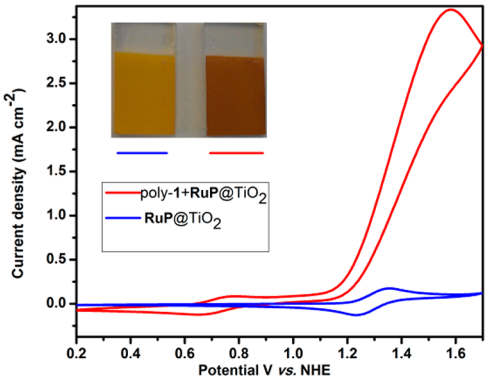

Figure 1. CV curves of poly-**1**+**RuP**@TiO_2 (red line) and **RuP**@TiO_2 (blue line) in pH 7 phosphate buffer (50 mM), scan rate 100 mV s^{-1}. Inset: poly-**1**+**RuP**@TiO_2 and **RuP**@TiO_2.

A three-electrode PEC cell was set up with the photoanode poly-**1**+**RuP**@TiO_2 as the working electrode, Ag/AgCl as the reference electrode, and Pt net as the counter electrode. First, linear scan voltammetry (LSV) experiments were carried out as shown in Figure 2. For poly-**1**+**RuP**@TiO_2 with light illumination, the photocurrent rapidly increased with the rise of applied potential from −0.25 to 0.20 V (vs NHE), and reached a plateau at E > 0.20 V with a photocurrent density of 1.4 mA cm^{-2}; this value is in agreement with our previously reported results.[15,16] For comparison, the **2**+**RuP**@TiO_2 electrode was also studied (Figure S11 in the Supporting Information), and it was found that it behaves very similarly to poly-**1**+**RuP**@TiO_2 with a current density of 1.5 mA cm^{-2} at about 2 V. These values are significantly higher in comparison to the current densities under dark conditions, indicating that the working electrodes are photoactive. Our results demonstrate that by using this straightforward polymerization method one can get photoactive electrode performance comparable to that of electrodes fabricated from the intricate coadsorption method.

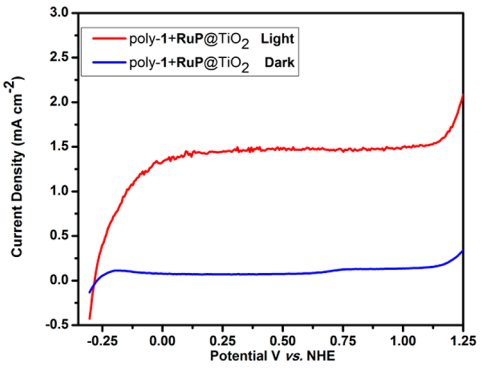

Figure 2. LSV measurements of the WEs under light illumination through a 400 nm long-pass filter (light intensity 300 mW cm^{-2}, scan rate 50 mV s^{-1}).

An experiment of transient current responses to on−off cycles of illumination on a poly-**1**+**RuP**@TiO_2 electrode under an external bias of 0.2 V vs NHE was then performed. As shown in Figure S13 in the Supporting Information, a remarkable initial photocurrent density of about 3.0 mA cm^{-2} was obtained by the poly-**1**+**RuP**@TiO_2 photoanode, while for the **RuP**@TiO_2 photoanode no significant photocurrent could be observed. The incident photo-to-current conversion efficiency (IPCE) spectrum of the poly-**1**+**RuP**@TiO_2 was measured (Figure S15 in the Supporting Information). A maximum IPCE value of 8.9% was observed at around 450 nm. After 500 s under light illumination, the photogenerated oxygen gas was confirmed by gas chromatography (GC) (Figure S16 in the Supporting Information). A total of 0.15 C of charge passed through the electrode while 0.32 μmol of O_2 was detected by GC, leading to a Faraday efficiency of 82%. However, the photocurrent from the poly-**1**+**RuP**@TiO_2 photoanode was found to be unstable with time. As shown in Figures S13 and S14a in the Supporting Information, the photocurrent density decreased from 1.4 to 0.3 mA cm^{-2} after 200 s of light illumination, respectively. For **2**+**RuP**@TiO_2 the photocurrent density decreased even faster. This stability problem is a general issue for all photoactive electrodes developed at the mo-

DOI: 10.1021/cs502115f
ACS Catal. 2015, 5, 3786−3790

ment.[15−17] Improvement of the durability of photoactive electrodes is urgently needed for further applications of these types of devices. From a comparison of the stabilities of poly-**1**+**RuP**@TiO_2 and poly-**1**@Fe_2O_3 (vide infra), together with the good stability of Ru(bda) on a carbon-based electrode,[21] the main reason responsible for the long-term photocurrent decrease was proposed to be the decomposition and/or desorption of the photosensitizer.

The photocurrent decay is most likely due to the following reasons. (1) Charge accumulation and recombination: under illumination, the charge accumulation occurs at the beginning, which can be considered as a charging process of the capacitance,[22] and then charge recombination occurs, leading to a fast photocurrent decrease in the first few seconds. (2) Inefficient mass transport: when a high photocurrent density is obtained on the mesoporous TiO_2 electrodes, O_2 bubbles are formed on the surface of the electrode, which blocks water access to the Ru catalyst. Meanwhile, the local pH value of the active site may decrease dramatically even with strong stirring, due to the inefficient mass/proton transport in mesoporous TiO_2. As a result, the driving force for water oxidation is reduced. Since charge transport and mass transport occur at the same time, these two reasons are most likely responsible for the initial fast decay of the photocurrent. (3) Decomposition and/or desorption of photosensitizer: in light-driven reactions, the rate-determining step (RDS) is not the oxidation of water by the catalyst, which is observed in other photosystems.[23] From the UV−vis spectrum (Figure S14b in the Supporting Information) of poly-**1**+**RuP**@TiO_2 after illumination, a new peak around 700 nm can be observed, which belongs to the absorbance of $Ru^{III}(bpy)_3$.[23,24] The DPV curves of poly-**1**+**RuP**@TiO_2 before and after illumination showed a significant peak current decrease (Figure S14c in the Supporting Information), which is due to the decomposition and/or desorption of **RuP**. Since the electron injection from dye into TiO_2 is ultrafast,[25] the color change is most likely due to ineffective electron transfer between the catalyst and photosensitizer, leading to the formation of the oxidized state of **RuP**. Therefore, the regeneration of **RuP** probably is the RDS. This will give photoproduced $\mathbf{Ru^{III}P}$ a chance to react with active oxygen and further lead to the decomposition or desorption of **RuP**,[26] which is probably the main reason for photocurrent decay under long-term illumination (vide infra).

To prove our hypothesis on the photocurrent decay, a series of experiments were conducted. First, a similar experiment was carried out in a higher concentration phosphate buffer solution (200 mM, pH 7.0) (Figure S17 in the Supporting Information). The photocurrent shows a slower initial decay in highly concentrated buffer due to its higher buffer capacity, indicating that inefficient proton transfer between the photonanode and bulk water is one of the reasons for the fast initial photocurrent decay. However, for long-term illumination the photocurrent still decays dramatically. Second, electrolysis experiments using poly-**1**+**RuP**@TiO_2 and **2**+**RuP**@TiO_2 as working electrodes were carried out at 1.5 V vs NHE. The electric-driven water oxidation by using poly-**1**+**RuP**@TiO_2 displayed a relatively more stable current density than **2**+**RuP**@TiO_2 (Figure S18 in the Supporting Information). This is in line with other reported work,[27] in which electropolymerization was also used to immobilize a water oxidation catalyst on metal oxide film and controlled-potential electrolysis showed sustained current. Poly-**1**+**RuP**@TiO_2 showed more stable current density under electric-driven condition in comparison to that under illumination. These phenomena imply that (i) the catalyst is robust and (ii) under light illumination, the photocurrent decrease is due to the decomposition/desorption of the photosensitizer **RuP**.

Kinetic isotope effects (KIEs) of poly-**1**+**RuP**@TiO_2 and **2**+**RuP**@TiO_2 were studied to reveal the RDS of our photoanodes during the catalytic processes. KIE reflects the kinetic information on water oxidation reactions and helps chemists interpret the RDS of the catalytic processes.[28−31] There are two different pathways for Ru-based water oxidation catalysts.[32] When the RDS is water nucleophilic attack pathway (eq 1), O−H bond cleavage is involved, the reaction shows a

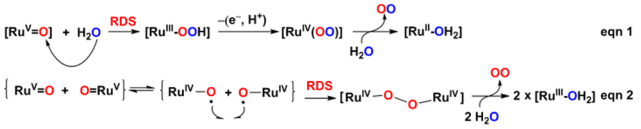

primary isotope effect, and the $KIE_{H/D}$ value is usually >2.[28−31] When the RDS is the dimerization of two Ru═O units (eq 2), no such cleavage is then involved and the reaction shows a secondary isotope effect ($KIE_{H/D}$ = 0.7−1.5).[33]

First, the electrocatalytic KIE of the poly-**1**+**RuP**@TiO_2 electrode was compared with that of **2**+**RuP**@TiO_2 under dark conditions in order to exclude the effect of photoinduced electron transfer. Chronoamperometric experiments were conducted in both H_2O and D_2O solutions with 100 mM Na_2SO_4 as the supporting electrolyte. On application of potentials on poly-**1**+**RuP**@TiO_2 the current densities showed negligible difference between H_2O and D_2O solutions (note that the applied potential 1.5 V vs NHE equals to the light-driving force $E(\mathbf{RuP}/\mathbf{RuP}^+)$ plus 0.2 V bias for water oxidation); the $KIE_{H/D}$ was calculated as ca. 1.1 (Figure 3a).

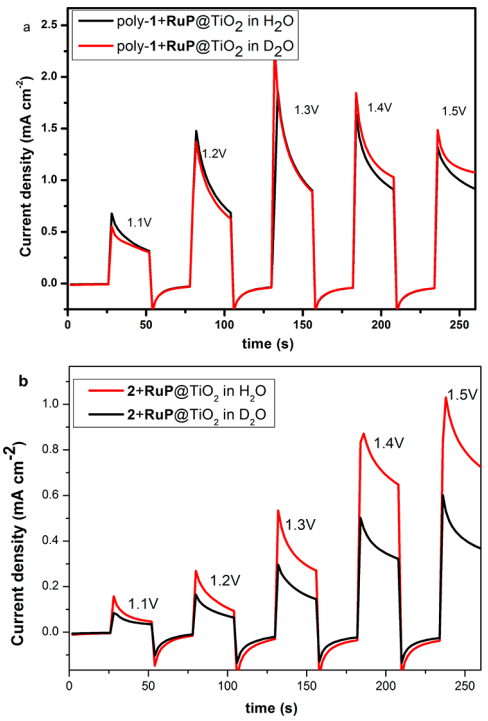

Figure 3. Chronoamperometric current densities measured in 100 mM Na_2SO_4 aqueous (H_2O or D_2O) solution under application of sequential potential steps.

DOI: 10.1021/cs502115f
ACS Catal. 2015, 5, 3786−3790

Under the same conditions, the **2**+**RuP**@TiO_2 electrode shows a $KIE_{H/D}$ of ca.1.9 (Figure 3b), which is significantly different from that of poly-**1**+**RuP**@TiO_2. Accordingly, poly-**1**+**RuP**@TiO_2 has a secondary isotope effect, and therefore poly-**1** was proposed to catalyze water oxidation through a radical coupling mechanism (eq 2). In contrast, the **2**+**RuP**@TiO_2 electrode had a primary isotope effect, and complex **2** was proposed to catalyze water oxidation via a water nucleophilic attack mechanism or mixed mechanisms. This difference is caused by the spatial distance between catalytic centers. As a polymer, the Ru centers of poly-**1** are apparently closer to each other; however, for catalyst **2**, although a flexible anchoring group is used, the Ru centers are most likely not close enough for the dimerization, resulting in catalyst **2** going through a water nucleophilic attack mechanism on the electrode surface.

In addition, the KIE experiments were also conducted under light illumination. The photocurrent of either poly-**1**+**RuP**@TiO_2 or **2**+**RuP**@TiO_2 (Figures S19 and S20 in the Supporting Information) showed no significant difference between H_2O and D_2O solutions under illumination, which means that the RDSs for both of the electrodes under light illumination are not related to the O−H bond cleavage. The result for **2**+**RuP**@TiO_2 seems contradictory to the KIE under electrocatalytic conditions. We believe, however, that the water oxidation mechanism under light illumination still remains the same as that under electrocatalytic conditions, i.e. water nucleophilic attack, but it is no longer a rate-limiting step. A reasonable explanation is that the regeneration of **RuP** becomes the rate-limiting step for the whole photoelectrochemical process for **2**+**RuP**@TiO_2. In another word, the KIEs of light-driven water oxidation by using poly-**1**+**RuP**@TiO_2 and **2**+**RuP**@TiO_2 electrodes reflect the RDS of the whole PEC process and are not limited to the catalytic cycle of water oxidation. This supports our speculation that the photoinduced electron transfer from catalysts to the oxidized **RuP** is not efficient enough. The photocurrent decay under long-term illumination is caused by slow regeneration of **RuP**, which can lead to the decomposition/desorption of **RuP**.

There are several strategies which can be used to avoid the photocurrent decay during long-term illumination: for instance, linking the catalyst and the photosensitizer together to improve the electron transport between catalyst and photosensitizer. Related work has been demonstrated by our group,[34] where catalyst and photosensitizer were linked by using bridging Zr^{4+} ions and a relatively stable photocurrent was obtained. Recently, Meyer et al. published a work where the same catalyst **1**, propylene carbonate, and photosensitizer were copolymerized on TiO_2;[35] a low photocurrent was achieved (40 μA cm^{-2}), but a relatively stable photocurrent could be obtained. Our results together with those of Meyer support that enhancing the electron transport between catalyst and photosensitizer will increase the stability of these types of PEC devices.

Another more straightforward strategy is to replace **RuP** by a more stable photosensitizer. Here we demonstrate our efforts on replacing **RuP**@TiO_2 by an α-Fe_2O_3 nanorod array in order to get a stable photocurrent. The α-Fe_2O_3 nanorod array serves as photosensitizer and semiconductor, at the same time, its morphology benefits for both mass transport and electron transfer can be compared with those of mesoporous TiO_2 (Figure S21 in the Supporting Information). Again, catalyst **1** was electrochemically polymerized on a Fe_2O_3 nanorod electrode. LSV experiments were carried out, and the results are shown in Figure S22 in the Supporting Information. At 0 V vs NHE both dark current and current under illumination have a small peak of Fe^{II}/Fe^{III},[36] and above 100 mV vs NHE the photocurrent increased with an increase in applied potential. An experiment of transient current responses to on−off cycles of illumination on a poly-**1**@Fe_2O_3 electrode under an external bias 0.6 V vs NHE was then performed as shown in Figure 4.

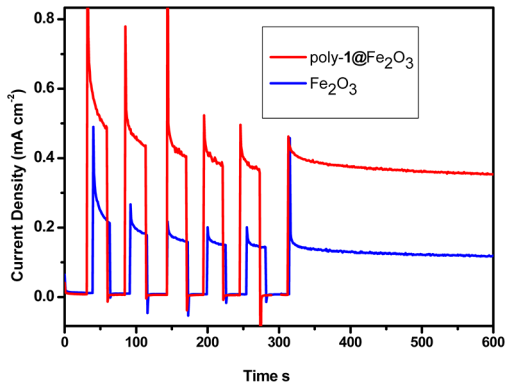

Figure 4. Transient current responses to on−off cycles of illumination on photoanodes under an applied potential of 0.6 V vs NHE in the three-electrode system PEC with Pt as the counter electrode, operated in a 50 mM pH 7.0 phosphate buffer solution.

An initial photocurrent density of 600 μA cm^{-2} was obtained by using poly-**1**@Fe_2O_3 photoanode; in comparison, the α-Fe_2O_3 nanorod electrode alone yielded an initial photocurrent density of 300 μA·cm^{-2}. For long-term illumination, a remarkably stable photocurrent of ca. 400 μA cm^{-2} can be obtained for the poly-**1**@Fe_2O_3 photoanode. Although the poly-**1**@Fe_2O_3 photoanode does not produce a photocurrent as high as that of poly-**1**+**RuP**@TiO_2, photosensitizer decomposition can be substantially suppressed by using α-Fe_2O_3 in comparison to **RuP**, and a stable photocurrent can be achieved.

In summary, the molecular Ru(bda) WOC catalyst **1** with 4-vinylpyridine as axial ligands has been successfully polymerized on a **RuP**-sensitized TiO_2 film, and a poly-**1**+**RuP**@TiO_2 electrode has been obtained. By using this electrode as the photoanode, a PEC device has been assembled in a three-electrode system. A high photocurrent density of ca.1.4 mA cm^{-2} has been achieved in a pH 7 phosphate buffer under a 0.2 V external bias. The KIE studies on poly-**1**+**RuP**@TiO_2 and **2**+**RuP**@TiO_2 suggest that poly-**1** undergoes water oxidation via a radical coupling mechanism and **2** on the electrode surface catalyzes water oxidation via a water nucleophilic attack pathway. For the photoelectrochemical reaction, the RDS is proposed to be the regeneration of **RuP**. When the dye-sensitized semiconductor **RuP**@TiO_2 is replaced with α-Fe_2O_3 semiconductor, a stable photocurrent (ca. 400 μA cm^{-2}) is obtained. From all experiments conducted, we can conclude that our molecular catalyst poly-**1** is an efficient and stable catalyst in PEC devices. However, the decomposition of the photosensitizer **RuP** limits the stability of the entire PEC devices. We hope that these results can inspire others in the design of more stable PEC devices for water splitting.

■ ASSOCIATED CONTENT

Supporting Information

The Supporting Information is available free of charge on the ACS Publications website at DOI: 10.1021/cs502115f.

DOI: 10.1021/cs502115f
ACS Catal. 2015, 5, 3786−3790

Synthesis of molecules, preparation of photoanodes, and NMR, SEM, EDX, and electrochemical measurement details (PDF)

AUTHOR INFORMATION

Corresponding Author

*E-mail for L.S.: lichengs@kth.se.

Notes

The authors declare no competing financial interest.

ACKNOWLEDGMENTS

We thank Dr. Hong Chen from Stockholm University for the SEM measurements of Fe_2O_3. We acknowledge the financial support of this work by the Swedish Energy Agency, the Knut and Alice Wallenberg Foundation, the Swedish Research Council, the National Natural Science Foundation of China (21120102036, 91233201), and the National Basic Research Program of China (973 program, 2014CB239402).

REFERENCES

(1) Gratzel, M. *Nature* **2001**, *414*, 338.
(2) Walter, M. G.; Warren, E. L.; McKone, J. R.; Boettcher, S. W.; Mi, Q.; Santori, E. A.; Lewis, N. S. *Chem. Rev.* **2010**, *110*, 6446.
(3) Tachibana, Y.; Vayssieres, L.; Durrant, J. R. *Nat. Photonics* **2012**, *6*, 511.
(4) Zong, R.; Thummel, R. P. *J. Am. Chem. Soc.* **2005**, *127*, 12802.
(5) Duan, L.; Xu, Y.; Tong, L.; Sun, L. *ChemSusChem* **2011**, *4*, 238.
(6) Wang, L.; Duan, L.; Stewart, B.; Pu, M.; Liu, J.; Privalov, T.; Sun, L. *J. Am. Chem. Soc.* **2012**, *134*, 18868.
(7) Alibabaei, L.; Brennaman, M. K.; Norris, M. R.; Kalanyan, B.; Song, W.; Losego, M. D.; Concepcion, J. J.; Binstead, R. A.; Parsons, G. N.; Meyer, T. J. *Proc. Natl. Acad. Sci. U. S. A.* **2013**, *110*, 20008.
(8) Ji, Z.; He, M.; Huang, Z.; Ozkan, U.; Wu, Y. *J. Am. Chem. Soc.* **2013**, *135*, 11696.
(9) Wang, L.; Duan, L.; Wang, Y.; Ahlquist, M. S. G.; Sun, L. *Chem. Commun.* **2014**, *50*, 12947.
(10) Duan, L.; Araujo, C. M.; Ahlquist, M. S. G.; Sun, L. *Proc. Natl. Acad. Sci. U. S. A.* **2012**, *109*, 15584.
(11) Duan, L.; Bozoglian, F.; Mandal, S.; Stewart, B.; Privalov, T.; Llobet, A.; Sun, L. *Nat. Chem.* **2012**, *4*, 418.
(12) Duan, L.; Fischer, A.; Xu, Y.; Sun, L. *J. Am. Chem. Soc.* **2009**, *131*, 10397.
(13) Jiang, Y.; Li, F.; Zhang, B.; Li, X.; Wang, X.; Huang, F.; Sun, L. *Angew. Chem., Int. Ed.* **2013**, *52*, 3398.
(14) Li, L.; Duan, L. L.; Xu, Y. H.; Gorlov, M.; Hagfeldt, A.; Sun, L. C. *Chem. Commun.* **2010**, *46*, 7307.
(15) Gao, Y.; Ding, X.; Liu, J. H.; Wang, L.; Lu, Z. K.; Li, L.; Sun, L. C. *J. Am. Chem. Soc.* **2013**, *135*, 4219.
(16) Gao, Y.; Zhang, L.; Ding, X.; Sun, L. *Phys. Chem. Chem. Phys.* **2014**, *16*, 12008.
(17) Zhang, L.; Gao, Y.; Ding, X.; Yu, Z.; Sun, L. *ChemSusChem* **2014**, *7*, 2801.
(18) Lapides, A. M.; Ashford, D. L.; Hanson, K.; Torelli, D. A.; Templeton, J. L.; Meyer, T. J. *J. Am. Chem. Soc.* **2013**, *135*, 15450.
(19) Wee, K.-R.; Brennaman, M. K.; Alibabaei, L.; Farnum, B. H.; Sherman, B.; Lapides, A. M.; Meyer, T. J. *J. Am. Chem. Soc.* **2014**, *136*, 8269.
(20) Fang, Z.; Keinan, S.; Alibabaei, L.; Luo, H.; Ito, A.; Meyer, T. J. *Angew. Chem.* **2014**, *126*, 4972.
(21) Li, F.; Zhang, B.; Li, X.; Jiang, Y.; Chen, L.; Li, Y.; Sun, L. *Angew. Chem., Int. Ed.* **2011**, *50*, 12276.
(22) Le Formal, F.; Sivula, K.; Grätzel, M. *J. Phys. Chem. C* **2012**, *116*, 26707.
(23) Lv, H.; Song, J.; Geletii, Y. V.; Vickers, J. W.; Sumliner, J. M.; Musaev, D. G.; Kögerler, P.; Zhuk, P. F.; Bacsa, J.; Zhu, G.; Hill, C. L. *J. Am. Chem. Soc.* **2014**, *136*, 9268.
(24) Leung, C.-F.; Ng, S.-M.; Ko, C.-C.; Man, W.-L.; Wu, J.; Chen, L.; Lau, T.-C. *Energy Environ. Sci.* **2012**, *5*, 7903.
(25) Bhasikuttan, A. C.; Suzuki, M.; Nakashima, S.; Okada, T. *J. Am. Chem. Soc.* **2002**, *124*, 8398.
(26) Hanson, K.; Brennaman, M. K.; Luo, H.; Glasson, C. R. K.; Concepcion, J. J.; Song, W.; Meyer, T. J. *ACS Appl. Mater. Interfaces* **2012**, *4*, 1462.
(27) Ashford, D. L.; Lapides, A. M.; Vannucci, A. K.; Hanson, K.; Torelli, D. A.; Harrison, D. P.; Templeton, J. L.; Meyer, T. J. *J. Am. Chem. Soc.* **2014**, *136*, 6578.
(28) Moonshiram, D.; Purohit, V.; Concepcion, J.; Meyer, T.; Pushkar, Y. *Materials* **2013**, *6*, 392.
(29) Yamada, H.; Siems, W. F.; Koike, T.; Hurst, J. K. *J. Am. Chem. Soc.* **2004**, *126*, 9786.
(30) Liu, F.; Concepcion, J. J.; Jurss, J. W.; Cardolaccia, T.; Templeton, J. L.; Meyer, T. J. *Inorg. Chem.* **2008**, *47*, 1727.
(31) Chen, Z.; Concepcion, J. J.; Hu, X.; Yang, W.; Hoertz, P. G.; Meyer, T. J. *Proc. Natl. Acad. Sci. U. S. A.* **2010**, *107*, 7225.
(32) Romain, S.; Vigara, L.; Llobet, A. *Acc. Chem. Res.* **2009**, *42*, 1944.
(33) Carey, F. A.; Sundberg, R. J. *Advanced Organic Chemistry: Part A: Structure and Mechanisms*; Springer: Berlin, 2007.
(34) Ding, X.; Gao, Y.; Zhang, L.; Yu, Z.; Liu, J.; Sun, L. *ACS Catal.* **2014**, *4*, 2347.
(35) Ashford, D. L.; Sherman, B. D.; Binstead, R. A.; Templeton, J. L.; Meyer, T. J. *Angew. Chem., Int. Ed.* **2015**, *54*, 4778.
(36) Sumathi, C.; Muthukumaran, P.; Radhakrishnan, S.; Ravi, G.; Wilson, J. *RSC Adv.* **2015**, *5*, 17888.

DOI: 10.1021/cs502115f
ACS Catal. 2015, 5, 3786−3790